

ORIGINAL ARTICLE

Memory-enhanced noiseless cross-phase modulation

Mahdi Hosseini¹, Stojan Rebić^{1,2}, Ben M Sparkes¹, Jason Twamley², Ben C Buchler¹ and Ping K Lam¹

Large nonlinearity at the single-photon level can pave the way for the implementation of universal quantum gates. However, realizing large and noiseless nonlinearity at such low light levels has been a great challenge for scientists in the past decade. Here, we propose a scheme that enables substantial nonlinear interaction between two light fields that are both stored in an atomic memory. Semiclassical and quantum simulations demonstrate the feasibility of achieving large cross-phase modulation (XPM) down to the single-photon level. The proposed scheme can be used to implement parity gates from which CNOT gates can be constructed. Furthermore, we present a proof of principle experimental demonstration of XPM between two optical pulses: one stored and one freely propagating through the memory medium.

Light: Science & Applications (2012) 1, e40; doi:10.1038/lisa.2012.40; published online 7 December 2012

Keywords: CNOT gate; cross-phase modulation; electromagnetically induced transparency; parity gate; quantum memory

INTRODUCTION

The optical Kerr effect is present in most materials but only becomes significant with very intense optical fields and/or long interaction times. In the limit of extreme nonlinearity, individual photons could be persuaded to interact strongly with one another and induce cross-phase modulation (XPM). This kind of interaction is a basis of the deterministic control-not gate and phase-not gates that lie at the heart of quantum computing algorithms.^{1,2} In addition, a large XPM can also be used for generation of cluster states, which are the basis for one-way quantum computing,^{3–5} as well as for implementation of nonlinear optical switches.⁶

To date, there have been various proposals aimed at realizing this strong interaction. Optical fibers are an attractive XPM medium.⁷ While they may not be highly nonlinear, the interaction times can be extended simply by using longer fibers. Unfortunately, the fast response time of optical fibers makes it impossible to temporally mode-match two copropagating single photons.⁸ Even if the nonlinearity is large, the fast response of the medium implies that only a small and randomly distributed portion of the single-photon wave packet experiences the phase shift.⁹ In the slow response regime, on the other hand, noise sources are always required to preserve the input/output canonical relations in nonlinear processes.^{9–11}

Another method of facilitating long interaction times for XPM is *via* light interaction with an atomic ensemble. Electromagnetically induced transparency (EIT)¹² based XPM exploits slow-light effects in an atomic ensemble to enhance the nonlinear interaction of light fields *via* the ac-Stark effect.¹³ It was shown that a phase shift ($\sim 10^{-5}$ rad) almost two orders of magnitude larger than that in optical fibers can be achieved using the EIT system.^{14,15} It has, however, been theoretically demonstrated that EIT-based XPM suffers from severe loss

in regimes where large phase shifts are expected. Gea-Banacloche¹⁶ showed that spontaneous emission into the initially unoccupied temporal modes is responsible for the small XPM in an EIT medium. In this scenario, a large phase shift is only possible in the limit in which the pulse bandwidth matches the medium bandwidth.¹⁶ The EIT medium in this regime, however, becomes ineffective and noisy. This is because some frequency components of one light field, lying outside the EIT window, can lead to spontaneous emission that is ultimately responsible for weak and low fidelity XPM. Moreover, the storage efficiency limit of 50%¹⁷ in EIT-based systems poses a practical limit on the fidelity of the output states.

In this paper, we propose a scheme based on storing two light fields *via* a Raman process in a Λ gradient echo memory (Λ -GEM).¹⁸ The simultaneous storage of the interacting light fields allows for greater interaction time than schemes where one field freely propagates through the memory medium.¹⁹ The nature of quantum memory in GEM is such that it stores different frequency components (modes) of the initial light pulse at different spatial locations. This property of the memory ensures that different modes at different spatial locations do not interact with one another. Thus, one can avoid the cross-mode spontaneous noise in XPM and multimode complications affecting the EIT-based systems outlined recently in Ref. 16. The medium bandwidth can be tuned to match the bandwidth of the probe field without otherwise changing the inherent nonlinearity of the system. This is because, all frequency components inside the broadened Raman profile experience the same absorption and therefore the loss due to the spontaneous emission for those frequencies will be negligible. We will start our discussion with an outline of the scheme and present results of our theoretical modeling. We then present a proof of principle experiment that shows XPM in a Λ -GEM system.

¹Centre for Quantum Computation and Communication Technology, Department of Quantum Science, The Australian National University, Canberra, Australia and ²Centre for Engineered Quantum Systems, Department of Physics & Astronomy, Macquarie University, North Ryde NSW 2109, Australia

Correspondence: Professor PK Lam, Centre for Quantum Computation and Communication Technology, Department of Quantum Science, Bld 38A, The Australian National University, Canberra ACT 0200, Australia.

E-mail: Ping.Lam@anu.edu.au

Received 9 May 2012; revised 12 July 2012; accepted 16 July 2012

MATERIALS AND METHODS

In Λ -GEM, a weak optical field is Raman coupled into the spin coherence of an ensemble of three-level atoms using a strong coupling field.¹⁸ A linearly varying ground-state splitting is applied using a magnetic field gradient, η , such that the light pulse is decomposed into its constituent Fourier components that are then stored longitudinally along the storage medium. Reversing the sign of the gradient will time-reverse the absorption leading to a coherent photon echo. This storage scheme has been proven to be versatile, efficient and noiseless.^{20–22}

To understand the dynamics in GEM, we use a polariton that is a superposition of the electric field, $\hat{\mathcal{E}}$, and atomic spin coherence, $\hat{\sigma}_{12}$, in the spatial Fourier domain,²³ defined as $\hat{\psi}(t, k) = k\hat{\mathcal{E}}(t, k) + \mathcal{N}\Omega_c / \Delta\hat{\sigma}_{12}(t, k)$, where k is the spatial frequency, \mathcal{N} is the effective linear atomic density, Δ is the Raman detuning from the excited state, and Ω_c is the coupling field Rabi frequency. During storage, the polariton evolves to higher k -values at a rate proportional to η . When using GEM for XPM, it is the polariton that will be phase shifted, leading to a phase shift of the photon echo on recall from the memory.

There are three properties of the polariton that are important to the following discussion:

- (i) The Fourier transform of the Maxwell equation gives $k\hat{\mathcal{E}}(t, k) = \mathcal{N}\hat{\sigma}_{12}(t, k)\Omega_c / \Delta$.²³ Because the spin coherence has a constant amplitude during storage, the Maxwell equation implies that \mathcal{E} is inversely proportional to k .
- (ii) The polariton can be stopped in k -space by switching η to 0. For a pulse stored with $\eta = 0$, the group velocity of the optical component is found to be $v_g = g\mathcal{N}/k^2(\Omega_c/\Delta)^2$.

- (iii) The polariton is purely atomic, $|\hat{\mathcal{E}}| = 0$, when the coupling field is off.

We will now analyze a scheme in which the probe and signal fields are simultaneously stored in a double-GEM system. Since the origin of this XPM is the ac-Stark effect, the effective phase shift can be enhanced by increasing the interaction time.

The Rb level structure and nonlinear interaction scheme between two photons stored inside the memory are shown in Figure 1a. The two fields (with Rabi frequencies of $g\mathcal{E}_p$ and $g\mathcal{E}_s$) are stored independently in two atomic spin coherences, $\hat{\sigma}_{12}$ and $\hat{\sigma}_{1'2'}$, using two coupling fields with Rabi frequencies of Ω_c and Ω'_c .

The probe and signal enter the medium consecutively. By timing the two coupling fields, each pulse is independently mapped into distinct polaritons. These modes propagate in opposite directions in k -space due to the opposite sign of the hyperfine Zeeman sub-levels. The k -space evolution of the two polaritons is stopped at a constant k by switching η to zero soon after the signal pulse enters the medium. The coupling field for the probe is then switched off, mapping the polariton into the spin coherence $\hat{\sigma}_{12}$. The coupling field for the signal is left on, ensuring a photonic component of this polariton that will give rise to an ac-Stark shift of the probe field polariton. The maximum available interaction time is proportional to the memory length and inversely to the group velocity of the signal light. After a controllable interaction time, the frequency gradient and coupling field Ω_c can be switched to recall the probe, which will be phase shifted due to the interaction with the signal. The interaction Hamiltonian of the system with level scheme depicted in Figure 1a can be written as:

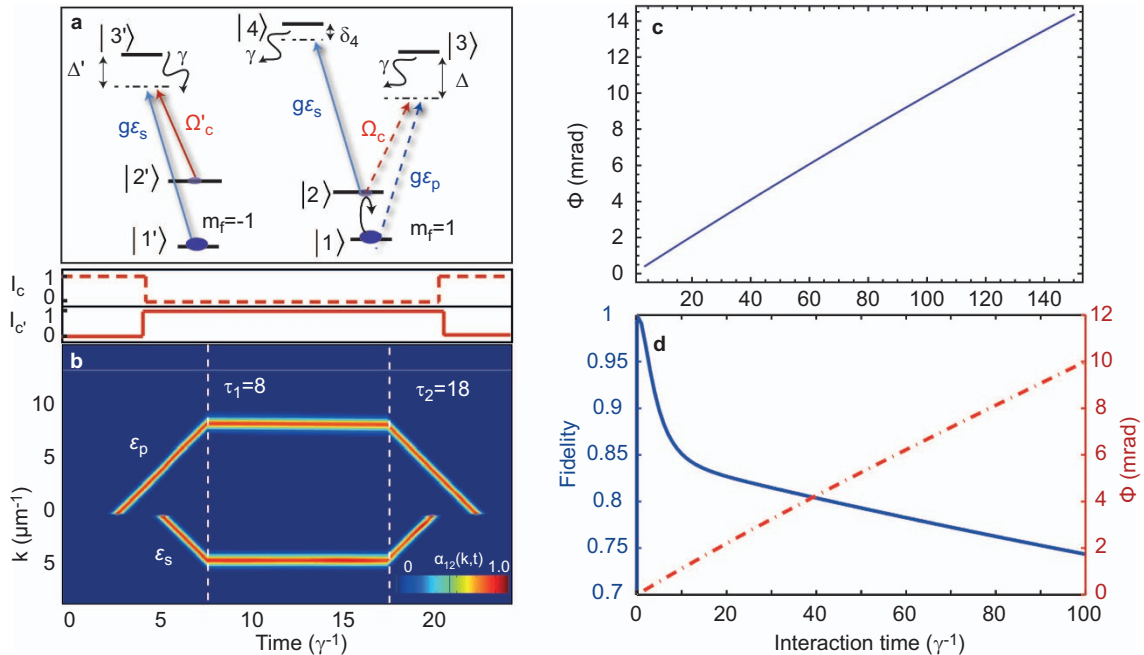


Figure 1 (a) Schematic atomic level structure of ^{87}Rb showing a scheme for the proposed nonlinear interaction. The probe \mathcal{E}_p and signal \mathcal{E}_s pulses arrived at different times are independently mapped to atomic coherence $|1\rangle\langle 2|$ and $|1'\rangle\langle 2'|$ using two coupling fields Ω_c and Ω'_c , respectively. The signal field can modify the phase of the atomic coherence $|1\rangle\langle 2|$ via the ac-Stark effect. (b) The total atomic coherence in spatial Fourier space (k) and time representing the evolution of two atomic fields in $k-t$ plane. The gradient field is switched off during $\tau_1 = 8/\gamma < t < \tau_2 = 18/\gamma$. The top part of the figure shows the coupling field switching protocols. (c) Semiclassical simulation results showing nonlinear phase shift between two coherent states with mean photon number of one as a function of interaction time. The following parameters were used: $\Omega_c = \Omega'_c = 10\gamma$, photon bandwidth $= \gamma$, $\Delta = \Delta' = 60\Omega_c$, $\delta_4 = 15\gamma$, $g = 0.085\gamma$ and number of atoms $N = 10^7$. (d) Results of quantum simulations for phase shift and phase gate fidelity as a function of interaction time. We assumed that the light is coupled to a seven-level atom with $g_{13} = g\sqrt{N}$, $g_{24} = g$, $g_{13'} = g\sqrt{N}$, and $\Omega_c = \Omega'_c = 20\gamma$. Other parameters are similar to the ones used in (c).

$$H_I = \frac{N}{L} \int \left[g \hat{\mathcal{E}}_p \hat{\sigma}_{31} + \Omega_c \hat{\sigma}_{32} + g \hat{\mathcal{E}}_s \hat{\sigma}_{42} + g \hat{\mathcal{E}}_s \hat{\sigma}_{3'1'} + \Omega'_c \hat{\sigma}_{3'2'} + H.c \right] dz \quad (1)$$

where $\hat{\sigma}_{ij}$ are the collective atomic spin operators, g is the atom–field coupling constant, N is total number of atoms in the interaction volume and L is the ensemble length. The phase of the coherence $\hat{\sigma}_{12}$ after the interaction time is then given by:

$$\phi_{\text{XPM}} = \int_{\tau_1}^{\tau_2} \frac{|g \hat{\mathcal{E}}_s(t - \tau_1)|^2 \delta_4}{2(\gamma^2 + \delta_4^2)} dt \quad (2)$$

and the loss rates of $\hat{\sigma}_{1'2'}$ and $\hat{\sigma}_{12}$ are given by $\gamma(\Omega'_c/\Delta')^2$ and $|g \hat{\mathcal{E}}_s(t - \tau_1)|^2 \gamma/(\gamma^2 + \delta_4^2)$, respectively.

RESULTS AND DISCUSSION

We numerically solve the Maxwell–Bloch equations to semiclassically model the storage and nonlinear interactions between two coherent states with mean photon number of one. The evolution of the signal and probe polaritons is shown in Figure 1b. The XPM resulted from nonlinear interaction between the signal and probe polaritons occurs during $\tau_1 < t < \tau_2$, when the gradient field is switched off. We have observed a linear increase in the phase of the retrieved probe field as a function of the signal field intensity. The simulation show no change in the phase of the probe field as its intensity increased, showing immunity to self-phase modulation (SPM).¹¹ The interaction strength is limited by the storage of the signal field which still has a non-zero group velocity in the memory. In order to increase the interaction strength and interaction time, one can use a pair of counter-propagating coupling fields to generate stationary light inside the memory. The application of a counter-propagating coupling field for the signal field would allow stationary trapping of the signal light. The physics of the trapping light in this case is similar to stationary light generated in an EIT medium that has previously been experimentally demonstrated.²⁴ The stationary light in GEM is generated through an off-resonance interaction and therefore suffers less from loss compared to EIT. The phase shift on the probe field due to the signal field is shown as a function of interaction time between them in Figure 1c. Similar results have been obtained for the phase shift of a strong coherent state ($\alpha \approx 10^2$) resulting from interaction with a signal pulse with mean photon number of one. Although the nonlinear phase shift for the proposed scheme is smaller than π , the current scheme can be used to implement parity or phase gates where the strength of the coherent states can offset the weakness of the nonlinearities.^{2,25} The simulation results suggest that $\alpha\theta > \pi$ is achievable in our scheme and therefore the error in discriminating the final states (even and odd parity states) can be less than 10^{-3} ,^{25,26} which is near-optimal.

We also perform quantum simulations by solving the master equation numerically. The interaction scheme in this case is simplified, so it can be solved using our available ultrafast computer. The quantum simulation, performed on the system during the interaction time ($\tau_1 < t < \tau_2$), yields useful information regarding the noise and gate imperfections. For this type of simulation, it is assumed that initially a photon is encoded in a coherence between $|1\rangle$ and $|2\rangle$ so the initial state of the atomic system becomes $\rho_{\text{at}} = 1/2(|1\rangle\langle 1| + |\psi_0\rangle\langle \psi_0|)$, where $|\psi_0\rangle = (|1\rangle + |2\rangle)/\sqrt{2}$. The initial state of the incoming signal photon is then given by $\rho_{\text{ph}} = |0_p, \psi_s\rangle\langle 0_p, \psi_s|$, where $|\psi_s\rangle = (|0_s\rangle + |1_s\rangle)/\sqrt{2}$, giving the total initial state $\rho(0) = \rho_{\text{at}} \otimes \rho_{\text{ph}}$. We also assume that the signal photon interaction is in the form of stationary light.

Next, we solve the master equation including Langevin noise terms. From the resulting density operator, the conditional phase shift

between a single photonic qubit in state $|\psi_s\rangle$ and polaritonic qubit encoded in the atomic coherence $|\psi_0\rangle$ is calculated as a function of interaction time. The conditional phase shift ϕ and gate fidelity are shown in Figure 1d for parameters closely corresponding to the semiclassical simulations. The fidelity calculated here is that of a two-qubit controlled phase gate using single photons.²⁷ This fidelity is low, as expected, since the interaction between single photons is very fragile. This is not such an issue for the parity gate described above since the interaction between a single photon and large coherent state is more robust against noise. Decoherence sources such as decay of the signal field amplitude due to Raman scattering (with lifetime of $\tau_{\text{sc}} \approx (\Delta/2\Omega)^2/\gamma \approx 200/\gamma$), spontaneous emission decay and atomic spin dephasing are included in the model. We found that the noise due to spontaneous emission is the dominant source of fidelity degradation.

Now we present proof of principle experimental results for nonlinear interaction between a stored coherent state and a propagating one. Although this experiment does not implement the full seven-level scheme outlined above, the results support our theoretical models with respect to the XPM strength and SPM properties. The experimental setup is shown in Figure 2a. A coupling field and a weak probe field were combined using a ring resonator and sent into a 20-cm long gas cell of ⁸⁷Rb mixed with 0.5 torr of Kr buffer gas. The gas cell was housed inside a pair of solenoids that generate switchable magnetic field gradients. After the memory, the coupling field was suppressed using a ⁸⁵Rb gas cell and the probe beam was measured using heterodyne detection (see Ref. 22 for more experimental details).

The probe was stored for approximately 15 μs , while the coupling field was switched off. During that time, a signal field generated from a diode laser and detuned by $\delta_3 \approx 2$ GHz from $F = 2 \rightarrow F' = 3$ of ⁸⁷Rb D_2 line was sent through the memory. This field was counter-propagating with respect to the probe and coupling fields to avoid measurement contamination. On recall, therefore, the stored probe field will be phase shifted proportional to the strength and duration of the signal field. To measure the size of the phase shift, we ran two storage experiments in succession, without and with the signal field, as shown in Figure 2b ((i) and (ii) respectively). A phase reference for the two recalled probe pulses was provided by a pulse that passed through the memory cell 10 μs before the start of each experiment. This reference pulse then allowed us to compare the recalled probe phase with and without the signal field, as indicated in the figure.

To verify that this phase shift is due to a nonlinearity in the memory, we measured the phase shift as a function of the signal field Rabi frequency, as shown in Figure 3a, where the solid line represents the theoretical expectation calculated¹⁹ using $\phi_{\text{XPM}} = \Omega_s^2 \delta_3 \tau / 2(\gamma^2 + \delta_3^2)$, where $\Omega_s = g|\mathcal{E}_s|$ is the signal field Rabi frequency and τ is its duration. As predicted by theory, our scheme has no measurable SPM, as shown in Figure 3b, where the recalled probe phase is seen to be independent of the probe intensity.

Based on the experimental data presented in Figure 3a, we estimate a phase shift on the order of 10^{-12} rad for signal and probe fields containing single photons. In our experiment, the large detuning of the signal field (2 GHz) severely reduces the available nonlinearity, but it is necessary due to the large Doppler broadening of thermal atoms. In fact, even with this detuning the scattering due to the signal field leads to substantial loss of the atomic coherence. In Figure 2b, for example, the probe recall is reduced from 53% to 7% by the signal field. In cold atomic ensembles,¹⁹ such as dipole trap systems, this detuning could be reduced by two orders of magnitude allowing two orders of magnitude larger phase shift. Performing the experiment in a confined

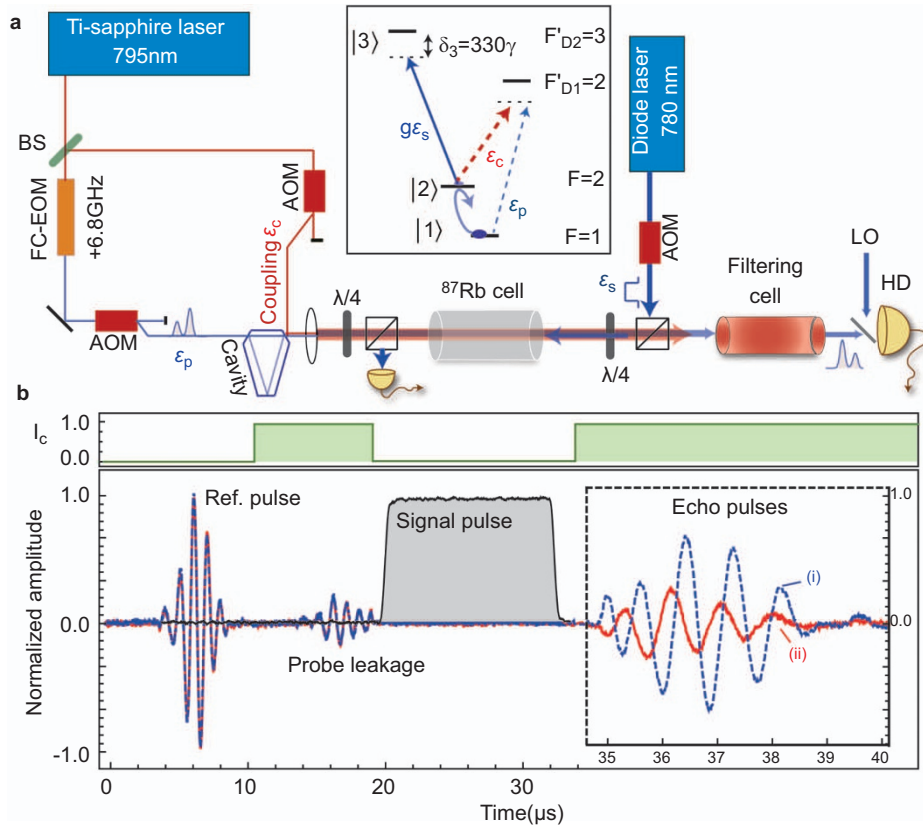


Figure 2 (a) Schematic experimental setup. The probe field (\mathcal{E}_p) is shifted by 6.8 GHz with respect to the coupling field (\mathcal{E}_c) using an FC-EOM and is combined with the coupling field using a ring cavity. The signal field (\mathcal{E}_s) is counter-propagating with other beams. The inset shows the atom–light interaction scheme. (b) Heterodyne data showing normalized amplitude of the modulated phase reference, input and echo probe pulses. The top trace shows the switching protocol of the coupling field intensity. Traces (i) (blue) and (ii) (red) show the amplitude of \mathcal{E}_p measured at the output of the memory without and with the signal pulse, respectively. Trace (ii) is taken 60 μ s after (i) and overlapped using the reference pulse as a timing signal. FC-EOM, fiber-coupled electro-optic modulator.

dipole trap system will also enhance the atom–light coupling strength by approximately three orders of magnitude due to the reduction in interaction volume, thus enhancing the phase shift by six order of magnitude. Furthermore, interaction of atomic spin with the stopped single photon wave packet (with duration of ~ 500 ns) instead of a freely propagating pulse of 10 μ s duration can in principle enhance the phase shift per single photon by nearly two orders of magnitude. Accounting for all these enhancement factors, our experimental results support the optimal predicted phase shift of 10 mrad. The predicted phase shift is orders of magnitude larger than that available in EIT systems.^{14,15}

CONCLUSIONS

In addition to the demonstrated efficient quantum storage and capability to arbitrarily manipulate optical pulses, the versatility of GEM can be extended to implement a parity gate from which CNOT gate can be constructed.²⁵ The lack of SPM and the demonstrated noiseless high efficiency storage in our scheme suggests that the proposed method is a potential candidate for implementing practical XPM between single photons and coherent states, as well as other applications in optical quantum technology. Further multimode analysis in Schrödinger picture is required to ensure that there is no obstacles in realization of this scheme.

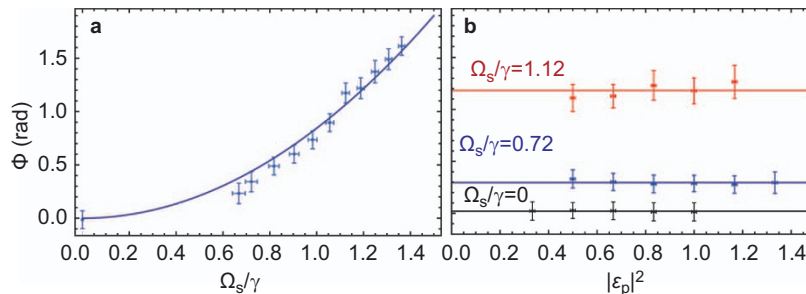


Figure 3 (a) Experimental results of nonlinear phase shift between two coherent states as a function of signal pulse Rabi frequency. The solid line is the predicted theory curve. (b) Phase shift for different signal pulse Rabi frequency as a function of peak intensity of the probe pulse normalized to the reference pulse.

ACKNOWLEDGMENTS

We thank John Close, Andrew White and André Carvalho for enlightening discussions. This research was conducted by the Australian Research Council Centre of Excellence for Quantum Computation and Communication Technology (CE110001027) and Centre of Excellence for Engineered Quantum Systems (CE110001013).

- 1 Milburn GJ. Quantum optical Fredkin gate. *Phys Rev Lett* 1989; **62**: 2124–2127.
- 2 Louis SG, Nemoto K, Munro WJ, Spiller TP. The efficiencies of generating cluster states with weak nonlinearities. *New J Phys* 2007; **9**: 193–220.
- 3 Briegel HJ, Raussendorf R. Persistent entanglement in arrays of interacting particles. *Phys Rev Lett* 2001; **86**: 910–913.
- 4 Raussendorf R, Briegel HJ. A one-way quantum computer. *Phys Rev Lett* 2001; **86**: 5188–5191.
- 5 Walther P, Resch KJ, Rudolph T, Schenck E, Weinfurter H *et al*. Experimental one-way quantum computing. *Nature* 2005; **434**: 169–176.
- 6 Williams WE, Soileau M, Stryland EWW. Optical switching and n_2 measurements in CS₂. *Opt Commun* 1984; **50**: 256–260.
- 7 Matsuda N, Shimizu R, Mitsumori Y, Kosaka H, Edamatsu K. Observation of optical-fibre Kerr nonlinearity at the single-photon level. *Nat Photon* 2010; **3**: 95–98.
- 8 Shapiro JH. Single-photon Kerr nonlinearity do not help quantum computation. *Phys Rev A* 2006; **73**: 062305.
- 9 Shapiro JH, Razavi M. Continuous-time cross-phase modulation and quantum computation. *New J Phys* 2007; **9**: 16–17.
- 10 Boivin L, Kartner FX, Haus HA. Analytical solution to the quantum field theory of self-phase modulation with a finite response time. *Phys Rev Lett* 1994; **73**: 240–243.
- 11 Joneckis LG, Shapiro JH. Quantum propagation in a Kerr medium: lossless, dispersionless fiber. *J Opt Soc Am B* 1993; **10**: 1102–1120.
- 12 Fleischhauer M, Lukin MD. Effect of large supersymmetric phases on Higgs production. *Phys Rev Lett* 2000; **84**: 22–25.
- 13 Schmidt H, Imamoglu A. Giant Kerr nonlinearities obtained by electromagnetically induced transparency. *Opt Lett* 1996; **21**: 1936–1938.
- 14 Lo HY, Chen YC, Su PC, Chen HC, Chen JX *et al*. Electromagnetically-induced-transparency-based cross-phase-modulation at attojoule levels. *Phys Rev A* 2011; **83**: 041804.
- 15 Shiau BW, Wu MC, Lin CC, Chen YC. Low-light-level cross-phase modulation with double slow light pulses. *Phys Rev Lett* 2011; **106**: 193006.
- 16 Gea-Banacloche J. Impossibility of large phase shifts via the giant Kerr effect with single-photon wave packets. *Phys Rev A* 2010; **81**: 043823.
- 17 Zhang S, Zhou S, Loy MMT, Wong GKL, Du S. Optical storage with electromagnetically induced transparency in a dense cold atomic ensemble. *Opt Lett* 2011; **36**: 4530–4532.
- 18 Hetet G, Longdell JJ, Alexander AL, Lam PK, Sellars MJ. Electro-optic quantum memory for light using two-level atoms. *Phys Rev Lett* 2008; **100**: 023601.
- 19 Chen YF, Wang CY, Wang SH, Yu IA. Low-light-level cross-phase-modulation based on stored light pulses. *Phys Rev Lett* 2006; **96**: 043603.
- 20 Hosseini M, Sparkes BM, Hetet G, Longdell JJ, Lam PK *et al*. Coherent optical pulse sequencer for quantum applications. *Nature* 2009; **461**: 241–245.
- 21 Hosseini M, Sparkes BM, Campbell G, Buchler BC, Lam PK. High efficiency coherent optical memory with warm rubidium vapour. *Nat Commun* 2010; **2**: 174.
- 22 Hosseini M, Sparkes BM, Campbell G, Lam PK, Buchler BC. Unconditional room temperature quantum memory. *Nat Phys* 2011; **7**: 794–798.
- 23 Hetet G, Longdell JJ, Sellars MJ, Lam PK, Buchler BC. Multimodal properties and dynamics of gradient echo quantum memory. *Phys Rev Lett* 2008; **101**: 203601.
- 24 Bajcsy M, Zibrov AS, Lukin MD. Stationary pulses of light in an atomic medium. *Nature* 2003; **426**: 638–641.
- 25 Munro WJ, Nemoto K, Spiller TP. Weak nonlinearities: a new route to optical quantum computation. *New J Phys* 2005; **7**: 137.
- 26 Nemoto K, Munro WJ. Nearly deterministic linear optical controlled-NOT gate. *Phys Rev Lett* 2004; **93**: 250502.
- 27 Yan XJ, Song PML, Song HS. Efficient implementation of the two-qubit controlled phase gate with cross-Kerr nonlinearity. *J Phys B* 2011; **44**: 025503.



This work is licensed under a Creative Commons Attribution-NonCommercial-NoDerivative Works 3.0 Unported License. To view a copy of this license, visit <http://creativecommons.org/licenses/by-nc-nd/3.0>